JAIST Repository
https://dspace.jaist.ac.jp/

Title	Flash-lamp-induced explosive crystallization of amorphous germanium films leaving behind periodic microstructures
Author(s)	Ohdaira, Keisuke; Matsumura, Hideki
Citation	Thin Solid Films, 524: 161-165
Issue Date	2012-10-23
Type	Journal Article
Text version	author
URL	http://hdl.handle.net/10119/10881
Rights	NOTICE: This is the author's version of a work accepted for publication by Elsevier. Keisuke Ohdaira, Hideki Matsumura, Thin Solid Films, 524, 2012, 161-165, http://dx.doi.org/10.1016/j.tsf.2012.10.023
Description	

JAIST
JAPAN
ADVANCED INSTITUTE OF
SCIENCE AND TECHNOLOGY

Japan Advanced Institute of Science and Technology

Flash-Lamp-Induced Explosive Crystallization of Amorphous Germanium Films Leaving Behind Periodic Microstructures

Keisuke Ohdaira[1,2] and Hideki Matsumura[1]

[1]Japan Advanced Institute of Science and Technology (JAIST)

1-1 Asahidai, Nomi, Ishikawa 923-1292, Japan

Phone: +81-761-51-1551, E-mail: ohdaira@jaist.ac.jp

[2]PRESTO, Japan Science and Technology Agency (JST)

4-1-8 Honcho Kawaguchi, Saitama 332-0012, Japan

Flash lamp annealing (FLA) can induce the explosive crystallization (EC) of micrometer-order-thick amorphous germanium (a-Ge) films. This EC leaves behind periodic microstructures consisting of two regions with different grain features existing alternatively along a lateral crystallization direction. One of the two regions contains a few hundred nm-sized relatively large grains, while such large-sized grains are not seen in the other region. This particular microstructure is similar to that of polycrystalline silicon (poly-Si) films formed through EC induced by FLA. The interval of the periodic structures in the polycrystalline Ge (poly-Ge) of 0.7-0.85 μm is smaller than that in the case of Si of about 1 μm. This is probably due to larger thermal diffusivity of a-Ge than that of a-Si. The speed of the EC is estimated to be 5-7 m/s, which is smaller than the speed of liquid-phase-epitaxy- (LPE-) based EC of ~8 m/s for Ge films reported previously. This fact indicates that a crystallization process other than LPE is

also involved in this EC, and solid-phase nucleation governs the EC. This is also similar to what have been previously confirmed in Si films, meaning that this particular EC could occur universally in a variety of materials.

Keywords: flash lamp annealing, explosive crystallization, polycrystalline germanium, periodic structure

1. Introduction

Non-thermal equilibrium annealing techniques have attracted significant attentions as the methods of forming device-quality films by crystallizing precursor amorphous films on low-cost substrates [1-12]. Of a number of rapid annealing techniques, flash lamp annealing (FLA) is of great advantage especially for forming photovoltaic crystalline films because of its millisecond-order annealing duration [9,10]. This enables us to sufficiently heat μm-order-thick amorphous films without the entire heating of substrates. We have so far found that FLA can induce the explosive crystallization (EC) of amorphous silicon (a-Si) films, self-catalytic lateral crystallization driven by the release of latent heat [13]. The lateral propagation speed of EC is on the order of m/s or more, by which we can fully suppress the diffusion of dopants inside Si films and hydrogen desorption from hydrogenated Si films [14,15]. These features are suitable for the fabrication of poly-Si solar cells. Interestingly, the flash-lamp-induced EC sometimes leaves behind periodic microstructures inside and on the surface of polycrystalline Si (poly-Si) films formed. This particular EC is observed especially when catalytic chemical vapor deposited (Cat-CVD) or sputtered a-Si films are used as precursor films [13,16,17]. Periodic surface roughness formed on flash-lamp-crystallized (FLC) poly-Si films through the particular EC can be utilized as anti-reflection structures [18]. Thus, the fundamental understanding of this curious EC is quite important to apply this technique to the production of photovoltaic materials, and we should investigate whether similar EC occurs also in other materials by FLA.

In this study, we have attempted the crystallization of amorphous germanium (a-Ge) films, instead of a-Si films, by FLA in order to know whether the particular EC can occur universally in extensive materials. Since germanium has lower melting

point than Si [11], crystallization under lower fluence and/or supporting substrate heating temperature can be expected. This would give us the broadening of the choices of substrate materials. Furthermore, the utilization of FLA to crystallize a-Ge films can lead to the formation of poly-Ge films with unique microstructures, unlike poly-Ge films formed by other techniques such as laser or metal-induced crystallization [12, 19-25]. Poly-Ge has been a promising material for application to devices such as thin-film transistors and solar cells [23-25], and the demonstration of crystallizing a-Ge films by FLA would present an alternative option to produce poly-Ge films.

2. Experimental Procedures

About 3-μm-thick a-Ge films were deposited directly on 20×20×0.7 mm^3-sized quartz glass substrates by sputtering at an Ar flow rate of 30 sccm, at a pressure of ~1 Pa, and at a RF power of 200 W, with no intentional substrate heating. a-Ge films then received a shot of quasi-5-ms flash lamp irradiation, consisting of discrete sub-pulses with tunable emission frequencies of 1-10 kHz. The irradiation of a series of quasi-millisecond pulse leads to the formation of macroscopic stripe patterns, visible to naked eyes, on the surface of crystallized materials. We can easily estimate lateral crystallization speed by dividing the width of the stripe patterns by the reciprocal of sub-pulse emission frequency [26]. In the case of Si, the velocity of EC leaving behind periodic microstructures is ~4 m/s, and the velocity of liquid-phase-epitaxy-(LPE-) based EC is ~14 m/s [26]. It should be noted that there is no impact of sub-pulse emission frequency on poly-Ge film properties, except for the width of the macroscopic stripe patterns. The spectrum of flash lamp light is shown in Fig. 1. The flash lamp pulse light has a broad spectrum mainly in a visible wavelength region.

The fluence of a quasi-5-ms flash lamp light was set to be about 9 J/cm^2, and no pre-heating was performed for Ge films during FLA. Crystallization and crystalline fraction of Ge films after FLA were evaluated by Raman spectroscopy using the 632.8nm line of a He-Ne laser. Due to the insufficient penetration depth (<100 nm) of the laser light, we also measured the Raman spectra of the poly-Ge films after wet etching using HF/HNO_3 solution. The surface morphology of FLC poly-Ge films were observed by scanning electron microscopy (SEM, Hitachi S-4100) operating at 20 kV. The cross-sectional microstructures of a FLC poly-Ge film were characterized by transmission electron microscopy (TEM, JEOL JEM-4000EX) at an operating voltage of 400kV. The cross-section of a FLC poly-Ge film was formed along an EC direction by focused ion beam (FIB, Hitachi FB2000A) at 30 kV.

3. Results

Figure 2 shows the surface image of a FLC poly-Ge film after FLA at a sub-pulse emission frequency of 3 kHz. One can see rainbow-like color on the surface of the FLC poly-Ge film. This is an indication of the existence of wavelength-order microstructures on the poly-Ge surface. We can also observe macroscopic stripe patterns on the FLC poly-Ge surface, as indicated by a pair of arrows on the figure, similar to the case of poly-Si after the irradiation of discrete sub-pulses [26]. From the width of the stripe pattern of ~2 mm and sub-pulse emission frequency of 3 kHz, a lateral crystallization speed is estimated to be 5-7 m/s. One can see a concentric pattern on the left side of the surface image. This is probably due to the ignition of EC at the center of the concentric pattern, and local microstructure inside a-Ge, such as a void, could be the trigger of starting EC. Figure 3(a) shows the Raman spectrum of an

as-sputtered precursor a-Ge film. A broad peak at around 270 cm^{-1}, originating from a-Ge phase, is clearly observed, and we cannot see any crystalline Ge (c-Ge) peaks. Figure 3(b) shows the Raman spectra of FLC poly-Ge films before and after wet etching and a single-crystalline Ge wafer for comparison. A sharp peak at ~300 cm^{-1} is seen in all the spectrum of the FLC poly-Ge films, whereas the signal of a-Ge is hardly observed. This clearly indicates the formation of a poly-Ge film with high crystalline fraction by a single shot of FLA. The full-width at half maximum (FWHM) of the c-Ge peak for at the FLC poly-Ge surface is ~5.0 cm^{-1}, which is significantly smaller than that of a reference Ge wafer of ~3.2 cm^{-1}. This means that FLC poly-Ge films consist of small grains [27]. Furthermore, the middle and bottom regions of the FLC poly-Ge films show even wider c-Ge Raman peaks with FWHMs of 6.3 and 6.7 cm^{-1}, respectively. This fact indicates that the surface region tends to contain larger grains. The c-Ge Raman peak of poly-Ge surface is located at a slightly higher wavenumber, which is a tendency opposite to results reported previously [22,27]. This is probably caused by compressive stress that precursor a-Ge films originally have and remains even after crystallization. The middle and bottom parts show slight low-wavenumber shift, which is also an indication of the existence of finer grains.

Figure 4 shows the surface SEM image of a FLC poly-Ge film. One can see microscopic periodic surface roughness along a lateral crystallization direction, and the interval of the periodic structure is 0.7-0.85 μm. This characteristic surface morphology probably creates the rainbow-colored surface shown in Fig. 2. Similar periodic surface morphology can also be seen on the surface of FLC poly-Si films, while the interval of the periodic structures is approximately 1 μm [13].

Figure 5(a) shows the bright-field cross-sectional TEM image of a FLC poly-Ge

film. It can be confirmed that not only a surface region but middle and bottom regions of the Ge film are crystallized. This is consistent with the result of Raman spectroscopy, shown in Fig. 3(b), and is reasonable because thermal diffusion length of a-Ge and glass during 5 ms is on the order of several tens of μm. The characteristic surface morphology with periodic roughness, shown in Fig. 4, is also observed in the TEM image. Furthermore, we can clearly see periodic structures also inside the poly-Ge film, in which two kinds of regions seem to appear alternatively along the crystallization direction. This feature can be seen more clearly in the dark-field image shown in Fig. 5(b). One of the two regions contains a few hundred nm-sized relatively large grains (large-grain region), while such large-sized grains are not seen in the other region (fine-grain region). The large-grain region includes surface protrusions, whereas the fine-grain region connects to surface concave parts. These features are also similarly seen in FLC poly-Si films [13,16,17]. Based on the TEM images, we can understand that the smaller FWHM of a c-Ge Raman peak for the surface of poly-Ge than inside, shown in Fig. 3(b), is due to the selective detection of surface protrusions containing larger grains. Figure 6 shows electron diffraction patterns acquired at the fine-grain and large-grain regions. A multi-spot diffraction pattern is obtained in the fine-grain region, and only limited numbers of spots are seen in the diffraction pattern of the large-grain region. These facts are consistent with the results of grain features confirmed in the TEM images shown above. Figures 7 and 8 show the high-resolution TEM images of the fine-grain and large-grain regions of the FLC poly-Ge film. We can actually observe a few nm-sized grains in the fine-grain region. On the contrary, no remarkable boundaries are seen in the lattice image of the large-grain region, clearly showing the formation of large grains.

4. Discussion

If EC occurs only through melting process, EC speed must be dominated by the speed of LPE at the melting point of precursor amorphous material. However, the EC speed of Ge films of 5-7 m/s, estimated from the width of macroscopic stripe patterns on FLC poly-Ge films, is smaller than that of LPE-based EC of ~8 m/s which was observed in an irradiation of 5-ns Nd:YAG laser pulse to a-Ge films preheated to temperatures of up till 870 °C [11]. This fact indicates that the EC observed in this study cannot be explained by simple liquid-phase EC, and we should probably consider a crystallization mechanism in which solid-phase process is involved. On the other hand, the formation of highly roughened surface on FLC poly-Ge films from flat a-Ge films is the clear evidence of melting-related crystallization. These facts probably suggest that both solid- and liquid-phase processes are included in the EC of a-Ge films observed in this study, as in the case of EC for Cat-CVD or sputtered CVD films [13,16,17]. The emergence of solid-phase crystallization can also be explained from the existence of 10-nm-sized fine grains. The EC velocity of 5-7 m/s and the interval of the microscopic periodic structure of 0.7-0.85 μm correspond to duration for the formation of one period of microstructure of roughly 100 ns. Since the density of 10-nm-sized fine grains is ~10^{18} /cm^3, nucleation rate of ~10^{25} /cm^{3}s is necessary. This value is possible only in solid-phase nucleation process [28], whereas cannot be realized in undercooled Ge melt at around the melting point of a-Ge [29], as in the case of Si [13].

Although similar microstructures are seen in FLC poly-Si and poly-Ge films, we can confirm some differences in them. One is the interval of microscopic periodic

structures: 0.7-0.85 μm for Ge and ~1 μm for Si. Since heat generation and thermal diffusion are involved in the EC process, differences between these values of Si and Ge should be discussed. The values of heat generation due to crystallization per unit volume in Ge and Si are almost same (~196 cal/cm^3) [30], and are not the cause of shortening the interval of the microstructure in FLC poly-Ge films. On the other hand, according to the values of thermal diffusion coefficient, density, and specific heat in literatures [10,31], the thermal diffusivity of a-Ge of 5.5×10^{-3} cm^2/s is larger than that of a-Si of 4.0×10^{-3} cm^2/s. This difference is not negligible and might affect the interval of the periodic microstructures. Further numerical investigation is needed to quantitatively understand the limiting factors of the periodicity of the microscopic structures.

Another curious difference in FLC poly-Si and poly-Ge films is the shape of grains in the large-grain regions. As has been reported previously, grains in the large-grain region of FLC poly-Si films are significantly stretched in a lateral crystallization direction [13,16,17], while grains in the large-grain region of FLC poly-Ge films have rather symmetric shapes. These phenomena can be understood as follows. In the case of Si, LPE speed has negative slope with respect to temperature at around the melting point of a-Si [10], meaning that the lower temperature of Si melt results in faster LPE. Since thermal gradient exists along a lateral crystallization direction during EC, grains in large-grain regions formed through LPE tends to be stretched. On the contrary, the LPE speed of Ge becomes smaller at lower temperatures around the melting point of a-Ge [11]. The lateral stretching of grains is therefore suppressed, and relatively symmetric-shaped grains are formed in the large-grain region of FLC poly-Ge films.

Finally, we discuss the possible advantages of using Ge for the precursor of FLA in photovoltaic applications. FLC poly-Ge films could be utilized in the bottom layers of tandem cells due to its small band-gap and resulting effective absorption of infra-red light. In fabricating tandem structures, the simultaneous crystallization of stacked a-Ge and a-Si films by FLA is probably possible. This is because EC is a high-speed lateral crystallization and there is no sufficient duration for the inter-diffusion of Si and Ge atoms. We have actually confirmed that p-i-n a-Si films can be crystallized by FLA with no remarkable change of the abrupt profiles of dopant atoms [14]. Another possible usage of Ge is the formation of FLC poly-SiGe alloy from a-SiGe precursor films. The difference of the interval of periodic microscopic structures in FLC poly-Si and poly-Ge films indicates the possibility of controlling the periodicity by tuning the composition of Si and Ge in precursor a-SiGe films. Periodic surface roughness in FLC films can be utilized as anti-reflection structures when they are used in substrate-type cells, as has been mentioned above [18]. Furthermore, if the FLC films are used in superstrate-type cells, the surface periodic structures of FLC films can be utilized as textured back reflectors. In these structures, the periodicity of the microstructures is quite effective to enhance light trapping [22], and the tuning of the periodicity by changing Ge contents in SiGe films would contribute to obtaining more photo-current in actual solar cells.

5. Summary

The EC of a-Ge films can leave behind periodic surface microstructures, similar to the case of the EC of Cat-CVD or sputtered a-Si films. Microstructures inside FLC poly-Ge films are also quite similar to those of FLC poly-Si films, which probably

indicates the emergence of EC in the same crystallization manner. These facts mean that this curious crystallization could occur universally in a variety of materials. FLC poly-Ge films have different spacing of the periodic structures compared to FLC poly-Si films, indicating the possibility of controlling the periodicity of microstructures by using a-SiGe alloy for precursors.

Acknowledgements

The authors acknowledge T. Yoshida and L. Yang of JAIST for their a-Ge film preparation and FLA experiment. This work was supported by JST PRESTO program.

References

[1] T. Yorimoto, S. Higashi, H. Kaku, T. Okada, H. Murakami, S. Miyazaki, T. Matsui, A. Masuda, M. Kondo, Jpn. J. Appl. Phys. 47 (2008) 6949.

[2] J. K. Saha, K. Haruta, M. Yeo, T. Koabayshi, H. Shirai, Sol. Energy. Mater. Sol. Cells 93 (2009) 1154.

[3] J. S. Im, H. J. Kim, Appl. Phys. Lett. 64 (1994) 2303.

[4] A.A.D.T. Adikaari, N.K. Mudugamuwa, S.R.P. Silva, Sol. Energy Mater. Sol. Cells 92 (2008) 634.

[5] H. Tsukamoto, H. Yamamoto, T. Noguchi, T. Suzuki, Jpn. J. Appl. Phys. 32 (1993) L967.

[6] R. Saleh, N.H. Nickel, J. Non-Cryst. Solids 338-340 (2004) 143.

[7] A. Hara, F. Takeuchi, N. Sasaki, J. Appl. Phys. 91 (2002) 708.

[8] C. C. Kuo, W. C. Yeh, J. F. Lee, J. Y. Jeng, Thin Solid Films 515 (2007) 8094.

[9] B. Pécz, L. Dobos, D. Panknin, W. Skorupa, C. Lioutas, N. Vouroutzis, Appl. Surf. Sci. 242 (2005) 185.

[10] M. Smith, R. McMahon, M. Voelskow, D. Panknin, W. Skorupa, J. Cryst. Growth 285 (2005) 249.

[11] C. Grigoropoulos, M. Rogers, S. H. Ko, A. A. Golovin, B. J. Matkowsky, Phys. Rev. B 73 (2006) 184125.

[12] W. Yeh, H. Chen, H. Huang, C. Hsiao, J. Jeng, Appl. Phys. Lett. 93 (2008) 094103.

[13] K. Ohdaira, T. Fujiwara, Y. Endo, S. Nishizaki, H. Matsumura, J. Appl. Phys. 106 (2009) 044907.

[14] K. Ohdaira, T. Fujiwara, Y. Endo, K. Shiba, H. Takemoto, S. Nishizaki, Y. R. Jang,

K. Nishioka, H. Matsumura, Proc. 33rd IEEE Photovoltaic Specialists Conf., (2008) 1690.

[15] K. Ohdaira, H. Takemoto, K. Shiba, H. Matsumura, Appl. Phys. Express 2 (2009) 061201.

[16] K. Ohdaira, S. Ishii, N. Tomura, H. Matsumura, Jpn. J. Appl. Phys. 50 (2011) 04DP01.

[17] K. Ohdaira, S. Ishii, N. Tomura, H. Matsumura, J. Nanosci. Nanotechnol. 12 (2012) 591.

[18] K. Ohdaira, T. Nishikawa, K. Shiba, H. Takemoto, H. Matsumura, Thin Solid Films 518 (2010) 6061.

[19] M. Uenuma, B. Zheng, T. Imazawa, M. Horita, T. Nishida, Y. Ishikawa, H. Watanabe, I. Yamashita, Y. Uraoka, Appl. Surf. Sci. 258 (2012) 3410.

[20] J. -H. Jeon, J.-Y. Choi,W.-W. Park, S.-W. Moon, S.-Ho Lim, S.-Hee Han, Proc. 2011 Nanotechnol. Mater. Devices Conf. (2011) 547.

[21] I. Chambouleyron, F. Fajardo, A. R. Zanatta, Appl. Phys. Lett. 79 (2001) 3233.

[22] K. Toko, I. Nakao, T. Sadoh, T. Noguchi, M. Miyao, Solid-State Electronics 53 (2009) 1159.

[23] T. Sadoh, H. Kamizuru, A. Kenjo, and M. Miyao, Appl. Phys. Lett. 89 (2006) 192114.

[24] C.-Y. Tsao, J. W. Weber, P. Campbell, G. Conibeer, D. Song, M. A. Green, Sol. Energy Mater. Sol. Cells 94 (2010) 1501.

[25] C.-Y. Tsao, J. W. Weber, P. Campbell, P. I. Widenborg, D. Song, M. A. Green, Appl. Surf. Sci. 255 (2009) 7028.

[26] K. Ohdaira, N. Tomura, S. Ishii, H. Matsumura, Electrochem. Solid-State Lett. 14

(2011) H372.

[27] S. Hayashi, M. Ito, H. Kanamori, Solid State Communications 44 (1982) 75.

[28] W. Marine and J. Marfaing, Phase Transitions 31 (1991) 299.

[29] A. Filipponi and M. Malvestuto, Meas. Sci. Technol. 14 (2003) 875.

[30] J. C C. Fan, H. Anderson, J. Appl. Phys. 52 (1981) 4003.

[31] W. Szyszko, F. Vega, C. N. Afonso, Appl. Phys. A 61 (1995) 141.

[32] O. Isabella, A. Campa, M.C.R. Heijna, W. Soppe, R. van Erven, R.H. Franken, H. Borg, M. Zeman, Proc. 23 rd European Photovoltaic Solar Energy Conf. (2008) 2320.

Figure captions

Fig. 1 The spectrum of flash lamp light used in this study.

Fig. 2 Surface of a FLC poly-Ge film formed with the irradiation of flash lamp light with duration of 5 ms and sub-pulse emission frequency of 3 kHz. One macroscopic stripe pattern is indicated by a pair of arrows.

Fig. 3 Raman spectrum of (a) a precursor a-Ge film and (b) FLC poly-Ge films before and after wet etching. The spectrum of a Ge wafer is also shown for comparison.

Fig. 4 Surface SEM image of a FLC poly-Ge film. An arrow indicates a lateral crystallization direction.

Fig. 5 (a) Bright-field and (b) dark-field cross-sectional TEM images of a FLC poly-Ge film. The cross-section was formed along a crystallization direction. Solid and dashed arrows close to the surface of the poly-Ge film on the bright-field image indicate large-grain and fine-grain regions, respectively.

Fig. 6 Electron diffraction patterns of FLC poly-Ge observed at positions "a" and "b" marked in Fig. 4(a).

Fig. 7 High-resolution TEM image of the fine-grain region of a FLC poly-Ge film.

Fig. 8 High-resolution TEM image of the large-grain region of a FLC poly-Ge film.

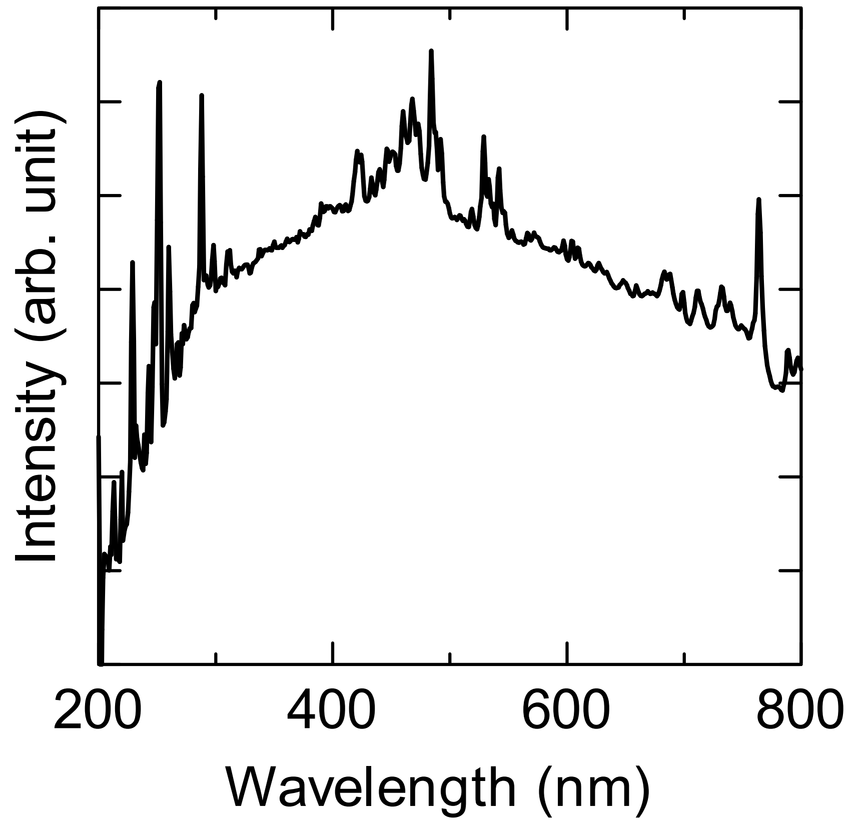

Figure 1 K. Ohdaira *et al.*,

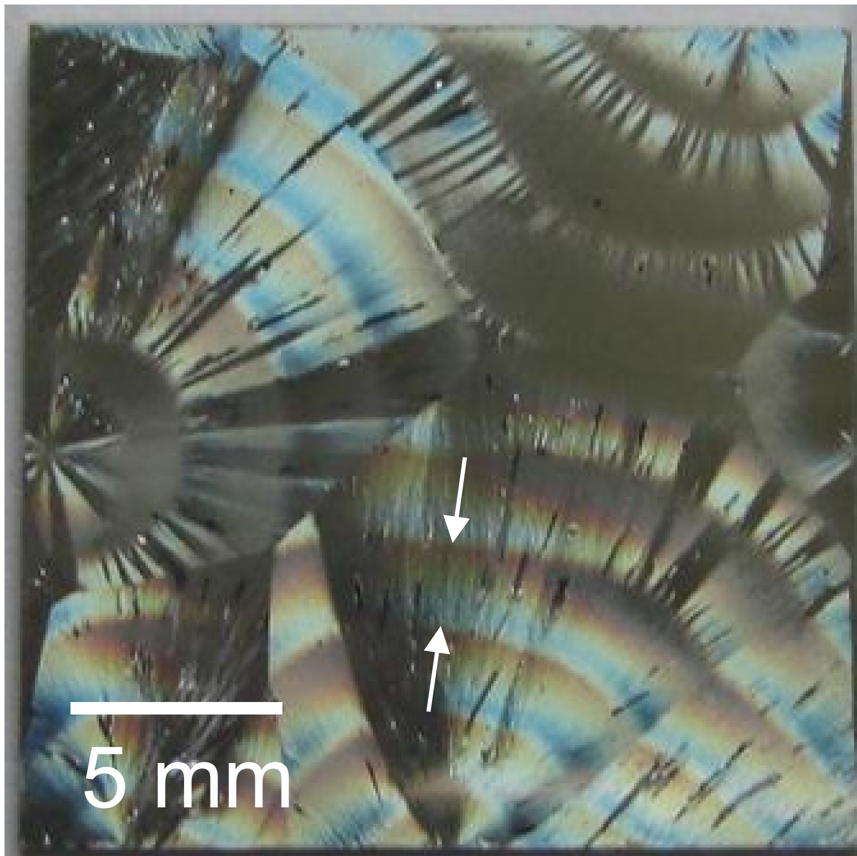

Figure 2 K. Ohdaira *et al*.,

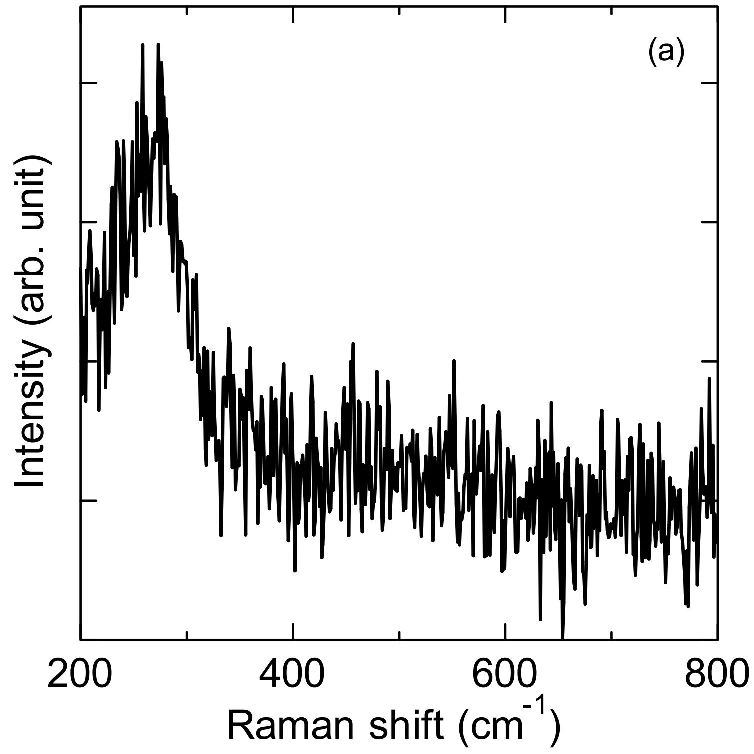

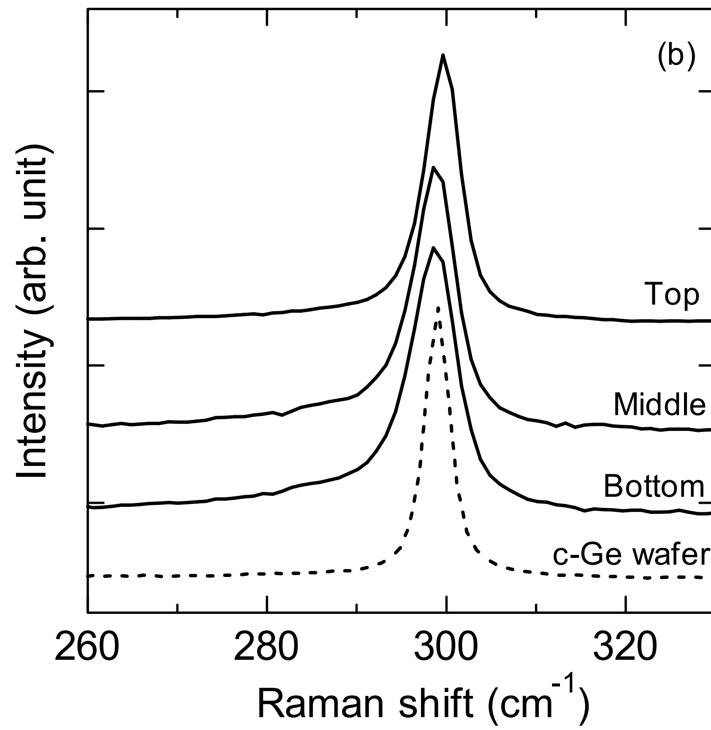

Figure 3 K. Ohdaira *et al.*,

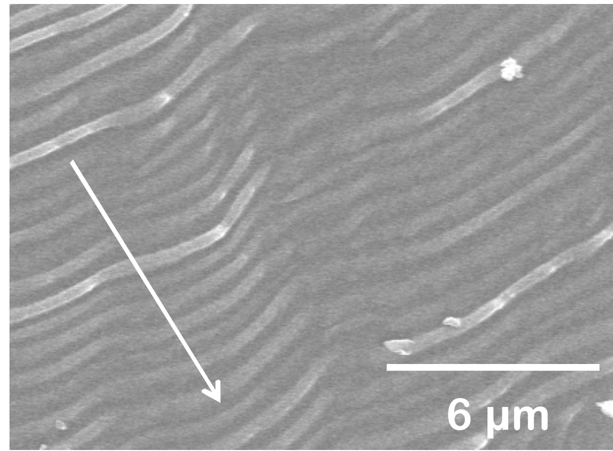

Figure 4 K. Ohdaira *et al*.,

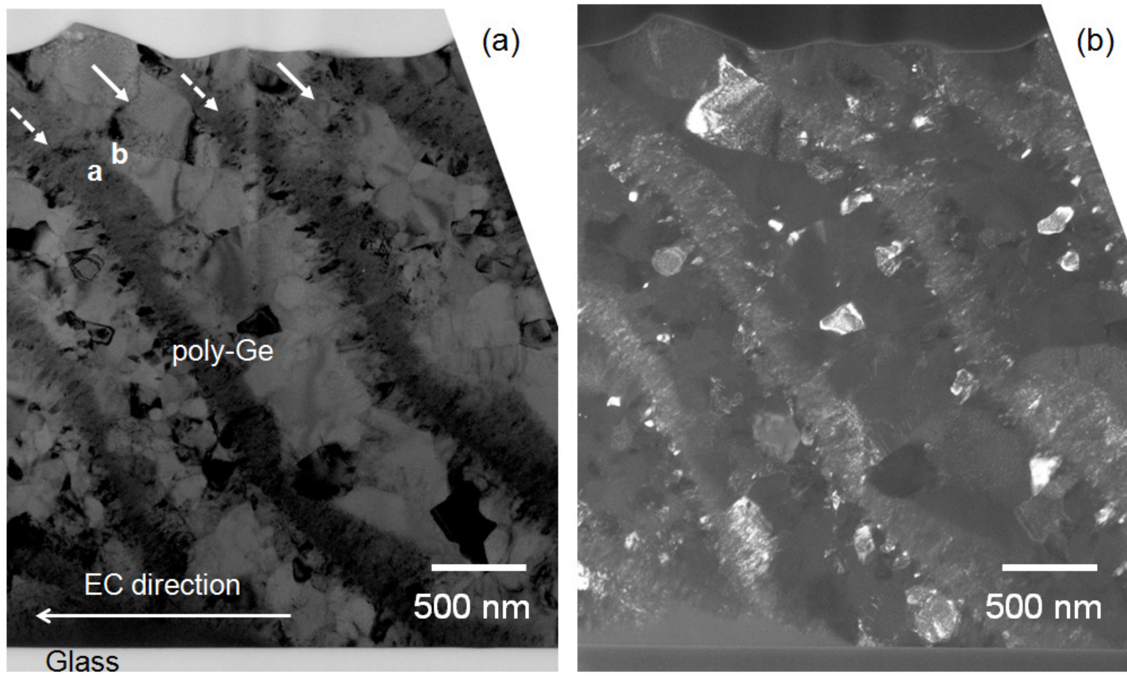

Figure 5 K. Ohdaira *et al*.,

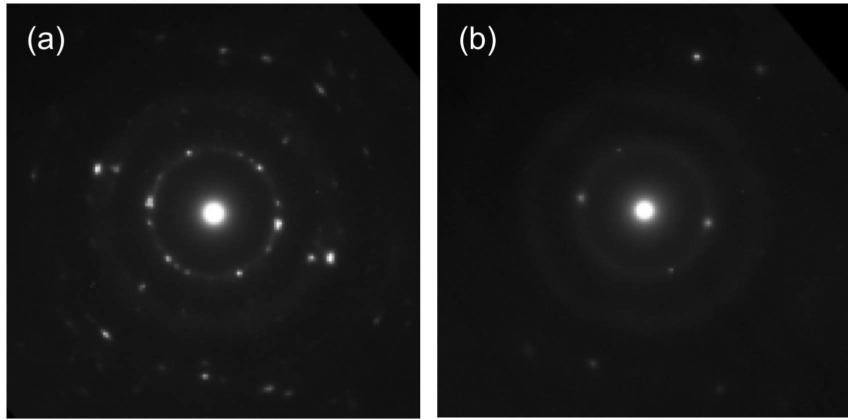

Figure 6 K. Ohdaira *et al*.,

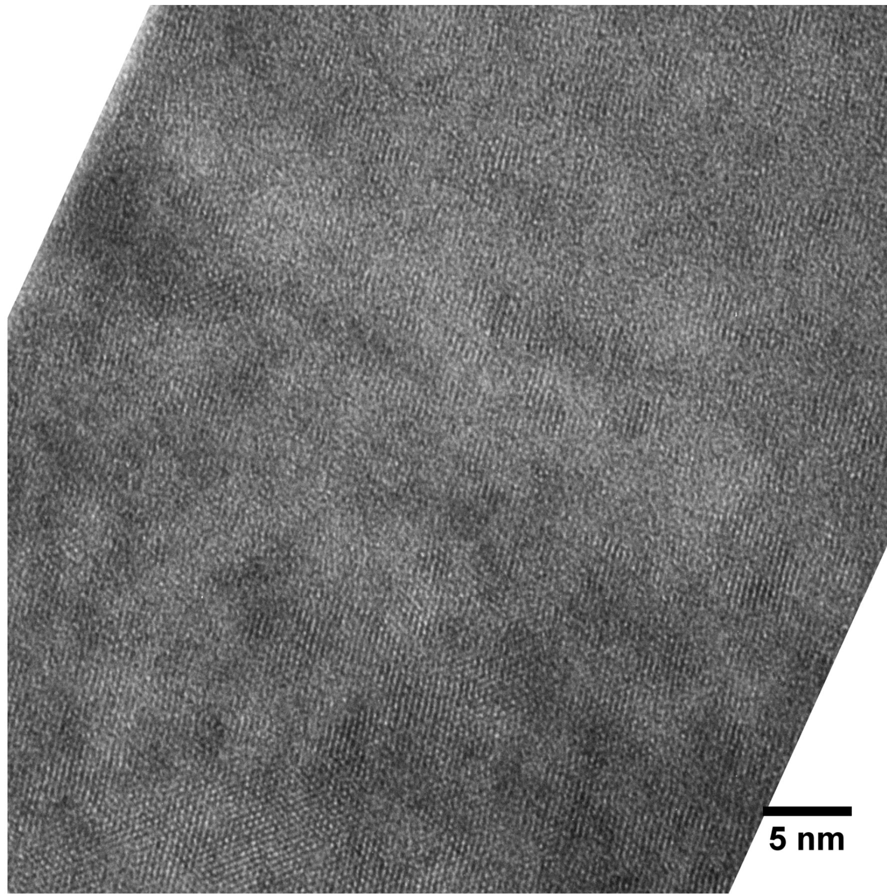

Figure 7 K. Ohdaira *et al*.,

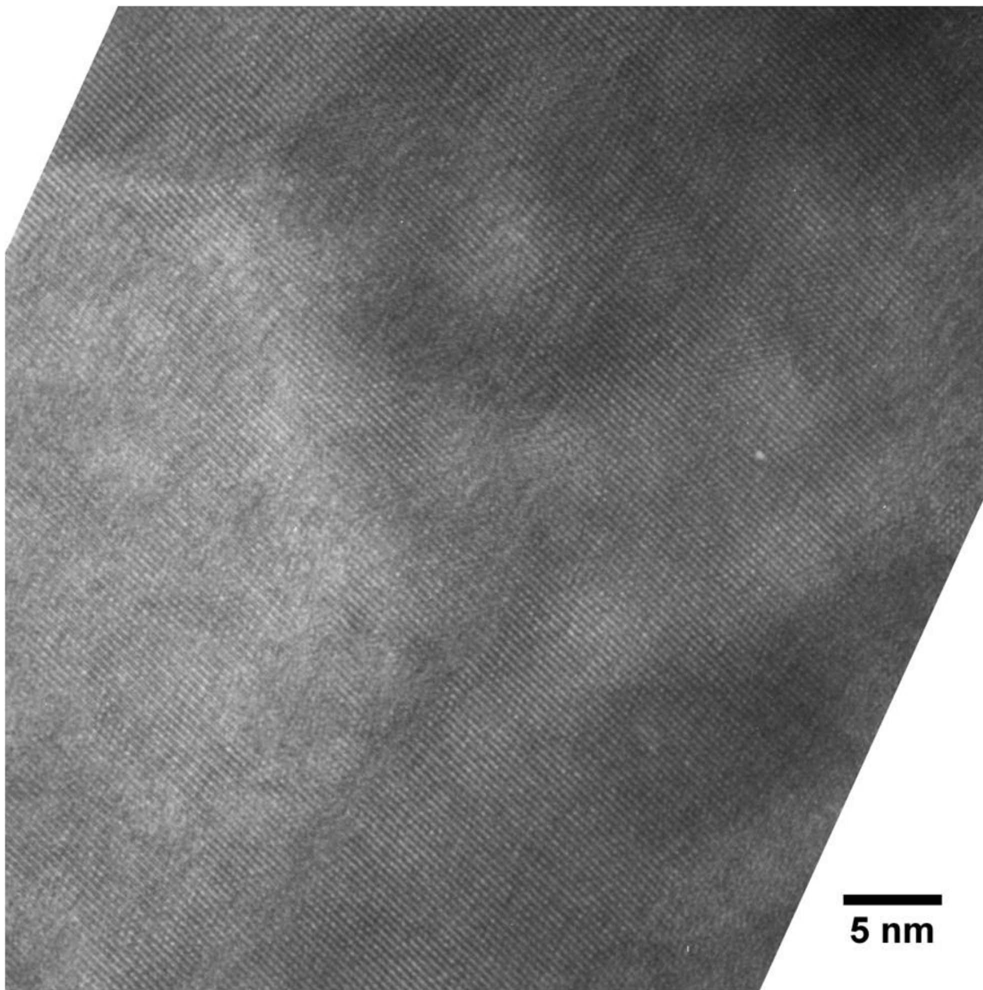

Figure 8 K. Ohdaira *et al*.,